12

Experimental Investigations into the Production Behavior of Methane Hydrate in Porous Sediment under Ethylene Glycol Injection and Hot Brine Stimulation

Xiao-Sen Li and Gang Li
Guangzhou Institute of Energy Conversion, Chinese Academy of Sciences
People's Republic of China

1. Introduction

Natural gas hydrates (NGH) are solid, non-stoichiometric compounds formed by host water molecules with small guest molecules, such as CH_4, C_2H_6, C_3H_8, CO_2, H_2S, etc (Sloan & Koh, 2008). Natural gas hydrate deposits involve mainly CH_4, and occur in the permafrost and in deep ocean sediment, where the necessary conditions of low temperature and high pressure exist for hydrate stability. Estimates of world hydrate reserves are very high, and vary from 0.2×10^{15} – 120×10^{15} m^3 of methane at STP (Standard Temperature and Pressure) (Sloan & Koh, 2008; Milkov, 2004; Klauda & Sandler, 2005). However, even with the most conservative estimates, it is clear that the energy in these hydrate deposits is likely to be significant compared to all other fossil fuel deposits, and was considered to be a potential strategic energy resource (Makogon et al., 2007; Collett, 2004; Moridis et al., 2009a).

Techniques for gas production from hydrate reservoir are based on three major dissociation principles, i.e.: 1) Depressurization (Yousif et al., 1991a; Moridis et al., 2004a; Moridis et al., 2007; Tang et al., 2007), to decrease the reservoir pressure below the hydrate dissociation pressure at a specified temperature; 2) Thermal stimulation (Kamath et al., 1991; Li et al., 2006, 2008a, 2008b; Tang et al., 2005a; Kawamura et al., 2007), to heat the reservoir above hydrate dissociation temperature with hot water, steam or hot brine injection; 3) Chemical inhibitor stimulation (Sira et al., 1990; Sung et al., 2002; Li et al., 2007a, 2007b; Kawamura et al., 2005a, 2005b), to inject chemicals, such as methanol or EG to shift the hydrate pressure-temperature equilibrium conditions. It is essential for safely and efficiently producing natural gas to characterize the hydrate dissociation mechanism and multiphase flowing mechanism of dissociated gas and water in hydrate-existing sediment.

Experimental investigations of hydrate dissociation behaviors under depressurization, thermal stimulation and chemical inhibitor stimulation in sediment have been reported. Yousif et al. (Yousif et al., 1990, 1991a, 1991b) developed a one-dimensional model to study depressurization-induced hydrate dissociation in berea sandstone cores suggested that a moving boundary model provide a satisfactory fit to hydrate dissociation measurements. Kono et al. (Kono et al., 2002) measured the dissociation rate of methane gas hydrate by

depressurizing method and derived the kinetic dissociation rate equation and the order of reaction. Tang et al. (Tang et al., 2005a, 2007) experimentally investigated the temperature distribution, gas and water production rate, and the thermal efficiency during the hydrate dissociation process using depressurization method and the hot water injection using a one-dimensional physical model. Sung et al. (Sung et al., 2003) examined the flowing characteristics of the dissociated gas and water from hydrate in porous rock by the depressurization and methanol injection schemes, using electric resistance to distinguish the hydrate formation and dissociation. Kamath et al. (Kamath et al., 1991) investigated the dissociation characteristics of the methane hydrates during the brine injection with low salt concentrations and high temperatures, and measured the effect of the temperature, the salinity, and the injection rate of the brine on the hydrate dissociation rate. Kawamura et al. (Kawamura et al., 2005a, 2005b, 2006) analyzed the dissociation behavior of an artificial hydrate core sample in methanol aqueous solution and the experiment was carried out by varying the temperature and concentration of the methanol aqueous solution. The dissociation kinetics of mixed gas hydrates that contain propane as a guest molecule has been investigated as well. Sira et al. (Sira et al., 1990) reported the characteristics of hydrate dissociation process during methanol and EG injection. They concluded that the rate of hydrate dissociation is a function of chemical concentration, injection rate, pressure, temperature of chemical solution and hydrate-chemical interfacial area. Li et al. (Li et al., 2007a, 2007b) experimentally investigated the gas production behavior from methane hydrate in porous sediment by injecting ethylene glycol (EG) solution with different concentrations and different injection rates. The results showed that the production efficiency is affected by both the EG concentration and the EG injection rate. The above experimental work focused on the characterization of hydrate dissociation during methanol and ethylene glycol injection, while few reports are found about the investigation of the dissociation behavior methane hydrate in the porous media under hot brine injection.

Among these methods, the thermal stimulation is capable of producing substantial amounts of natural gas, and it will be more effective combining with the depressurization or the chemical injection methods. (Moridis et al., 2003, 2004b, 2009b) So far, the impacts of the higher concentrations (0~24 wt%) of the injected brine solution at a wide temperature ranges (-1~130 ^{o}C) are not well understood yet, especially at the medium temperature ranges. And ethylene glycol (EG) is widely known as a thermodynamic inhibitor of gas hydrate, studies of natural gas dissociation in the presence of EG are limited, especially the impacts of the EG concentration and injection rate on hydrate dissociation are not well understood yet (Sira et al., 1990; Li et al., 2007a; Kawamura et al., 2005a).

In this work, the production behaviors of MH in unconsolidated sediment under hot brine and EG injection were investigated in a developed one-dimensional experimental apparatus. In the experiments of the hot brine injection, NaCl aqueous solution with the concentration of 0~24 wt% and the temperature of -1~130 ^{o}C was injected into the vessel with the injection rate of 9.99ml/min. The dissociation kinetics of methane hydrate in porous sediment, the production behaviors of gas and water, and the thermal and the energy efficiencies of the hydrate recovery process under hot brine injection were investigated. The experiments of the EG injection were carried out by varying the concentration and injection rate of the EG solution. The relationship between these two parameters and the production behavior was obtained. In addition, the efficiency of the gas production process during MH dissociation was determined.

2. Experimental Apparatus

The schematic diagram for the one-dimensional experimental apparatus used in this work is shown in Figure 1. The pressure vessel was immersed in an air bath with the temperature range from -20 °C to 80 °C, ±0.5 °C to maintain a constant temperature. The vessel is made of quartz glass and has an internal diameter of 30mm and a length of 534mm, and it can be operated up to 10MPa. Four resistance thermometers and two pressure sensors with three differential pressure transducers were uniformly-spaced, shown in Figure 1, to measure the temperature and pressure profile along the vessel. The thermometers are Pt100 with the range of -20 °C to 200 °C, ±0.1 °C. The pressure transducers are KELLER PA-21S 80400, 0-20MPa, ±0.25%. Two gas flow meters, which were used to measure the gas injection or production rate and the cumulative gas produced from the vessel, are both of D07-11A/ZM, 0-1000 ml/min, ±1% from "seven star company". The pressure transducers, thermometers, gas flow meters, were calibrated using a pressure test gauge with the error of ±0.05%, a mercury thermometer with the tolerance of ±0.01 °C, and a wet gas meter with the accuracy of ±10 ml/min, respectively. The two balances, which were are used to measure the rates of liquid input and output, respectively, are Sartorius BS 2202S, 0-2200g, ±0.01g. In order to protect the metering pump from corrosion by the hot brine or chemical inhibitors, the middle containers have been used for the solution injection. The data acquisition system records pressure, differential pressure, temperature, gas/water injection rate and production rate. The vessel and the loading pipelines were covered from a heat-insulating material to avoid the heat loss during brine injection. The NaCl used was analytically pure supplied by Guangzhou Chemical Reagent Factory, China. The EG was analytically pure, and the methane gas was produced by Foshan Kody Gas Chemical Industry Co., Ltd, China with its purity of 99.99%.

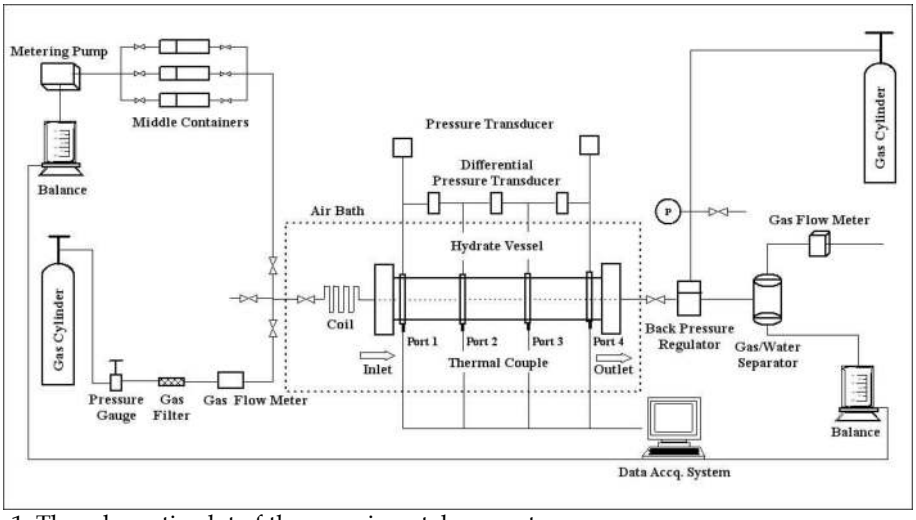

Fig. 1. The schematic plot of the experimental apparatus

3. Hot brine stimulation

3.1 Experimental Procedures

During the experiment, the raw dry quartz sand with the size range of 300-450 μm are tightly packed in the vessel, and then the vessel was evacuated twice to remove air in it with a vacuum pump. NaCl aqueous solution with the concentration of 2 wt% instead of distilled water was used for all experiments because of the higher formation rate of brine solution than that of the distilled water in sediments. (Tang et al., 2005b) Hence, in this work the dry quartz sand in the vessel was wetted at atmospheric pressure with 2 wt% NaCl aqueous solution, which was injected into the vessel from a the middle containers with a metering pump, when the amount of the liquid driven from the vessel was equal to those injected. Then the methane gas was injected into the vessel up to the pressure, which reached much higher than the equilibrium hydrate formation pressure at the working temperature. After that, the vessel was closed as an isochoric system, and the temperature in the vessel was gradually decreased to form the hydrate by changing the air bath temperature. In this work, the temperature of the air bath during the hdyrate formation is 0 ^{o}C. It was considered that the formation had not completed until there was no pressure decrease in the vessel.

Runs	T before formation ^{o}C	P before formation MPa	P before injection MPa	T of injected brine ^{o}C	Brine injected wt%
H1	25.7	5.898	3.041	130	0
H2	23.2	5.635	3.022		8
H3	20.3	5.617	3.095		16
H4	24.3	5.641	3.097		24
H5	25.2	5.641	2.973	90	0
H6	25.5	5.904	3.052		8
H7	28.7	5.849	3.095		16
H8	26.3	5.849	3.102		24
H9	24.0	5.922	2.888	50	0
H10	27.4	5.825	2.961		8
H11	28.8	5.934	2.955		16
H12	28.8	6.251	3.01		24
H13	27.5	6.013	2.967	-1	2
H14	27.8	6.007	3.047		8
H15	26.4	5.916	3.113		16
H16	26.2	5.507	2.845		24

Table 1. Experimental conditions of MH dissociation by hot Brine injection

Methane hydrate dissociation under hot brine injection was carried out in the following procedures. The brine with certain concentration was prepared in the middle container. The back pressure regulator was set to the certain required pressure value, which is the system pressure during the hydrate dissociation process under hot brine injection. The brine was firstly heated or cooled by the heater/cooler in the middle container. Then the brine was injected into the vessel. After a few minutes, gas and liquid began to release from the vessel through the outlet valve. During the entire formation and the dissociation runs of methane hydrate, the data thus as the temperature and the pressure in the vessel, the gas production, the amount of injected brine, and the liquid production were recorded at 6 second intervals. The brine injection rate is 9.99 ml/min. The detailed experimental arrangement is shown in Table 1.

3.2 Hydrate Dissociation

In this work, a total of 16 experimental runs were carried out to investigate into the dissociation behaviors of methane hydrate in the porous media by injecting the aqueous solutions of NaCl at -1, 50, 90 and 130 ^{o}C, respectively, and with the injection rate of 9.99 ml/min, as shown in Table 1.

In Run H1-Run H12, brine solutions were with 0, 8, 16 and 24 wt%, respectively. In Run H1, Run H5 and Run H9, the methane hydrate was dissociated with the effect of hot water (0 wt% brine solution) at 50, 90 and 130 ^{o}C, respectively. In Run H13- Run H16, the methane hydrate was stimulated with the brine solution with the concentrations of 2, 8, 16 and 24 wt%, respectively, and at -1 ^{o}C, lower than that of the hydrate system in the vessel (0 ^{o}C). Since the hydrate in the sediment in the vessel from 2 wt% NaCl solution was formed at 0 ^{o}C when, as did in Run H13, the brine was injected at 2 wt% and -1 ^{o}C into the vessel, the hydrate was not dissociated from the brine solution. Hence, the purpose of Run H13 is to determine the amount of free gas in the vessel. In addition, in Run H14-Run H16, .the hydrate was dissociated on account of the effect of the brine solution without thermal effect. In other experimental runs, the hydrate was dissociated from the synergistic effect of the heat and salt.

In this work, the following processes were involved, brine replacement of pore solution, heat transfer, and ion diffusion accompanying brine injection. Among these processes, the high salinity or high temperature can cause hydrate dissociate by shifting hydrate outside its stability regime. The high salinity can result either by the direct replacement of the original pore solution with high concentration of brine or by the diffusion of ions due to a concentration gradient, and the high temperature can be caused either by the direct replacement of the original pore solution with high temperature brine or by thermal transfer due to a temperature gradient.

3.2.1 Hot water stimulation

Figure 2 shows the curve of the temperature change with time at Port 2, Port 3 and Port 4 (the outlet) in the vessel with the injection of hot water at 50, 90 and 130 ^{o}C, respectively, as did in Run H9, Run H5 and Run H1. As shown in Figure 2, each temperature curve consists of the horizontal section and the ascending section. The horizontal section represents the hydrate non-dissociation processes and the isothermally endothermal dissociation processes resulting from the direct replacement of the original pore solution and heat transfer from

hot water; the ascending section is the heterothermally endothermal process of the system in the porous media in the effect of hot water after the hydrate dissociation has fully completed. As shown in Figure 2, in the above three runs, the dissociation firstly happened in the inlet of the vessel, and then in Port 2, Port 3 and Port 4 with time in turn until the hydrate in the vessel was completely dissociated. Accordingly, it is considered that the dissociation process of the hydrate in the vessel is the moving-forward process of the hydrate dissociation boundary from the inlet to the outlet. In other words, the flowing of hot water injected in the vessel can be regarded as the moving of a piston from the inlet to the outlet.

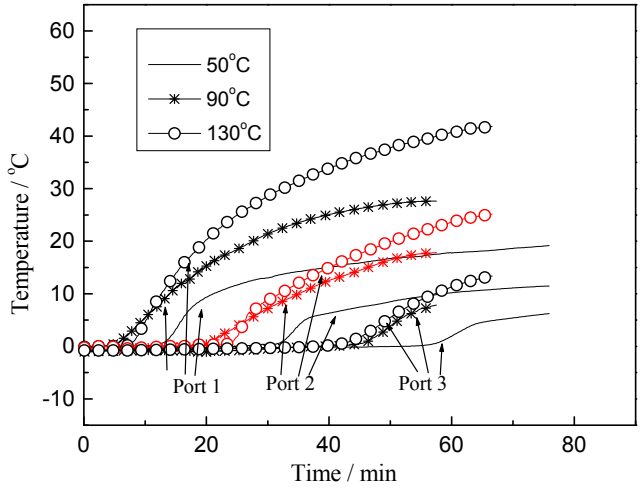

Fig. 1. The curve of the temperature change over time at Ports 1-3 in the vessel in Run H1, Run H5 and Run H9 with the effect of hot water at 50 °C, 90 °C and 130 °C

3.2.2 Brine stimulation

In Run H13-Run H16, the experiments of the brine stimulation was carried out. Figure 3 shows the curve of the temperature change over time at Port 4 in the vessel with the injection of the brine solution at -1 °C with 2, 8, 16 and 24 wt%, respectively. For Prot 1 and Port 3, the characteristics of the curve of the temperature change over time are similar. Since in the above experiments, the brine solution was injected into the vessel at -1 °C, lower than that of the hydrate system in the vessel (0 °C), the hydrate dissociation can be only caused from the inhibitors, not from the thermal effect.

As shown in Figure 3 and discussed above, under the injection of the brine at 2 wt% and -1 °C into the vessel, the hydrate was not dissociated. However, the hydrate dissociation can be caused by the effect of the brine solution with higher concentrations. As shown in Figure 3, the process of the hydrate dissociation is the process of the temperature decrease, which is the result of the presence of the brine solution. Since the temperature drop was caused by the heat balance between that needed for hydrate dissociation and that supplied from

surrounding environment, the lowest point of temperature represents the occasion when hydrate dissociated most intensely. In addition, it was found that the time for the hydrate dissociation is shortened and the degree of depth (well depth) of the temperature drop increases with the increase of the concentration of the brine solution.

According to the calculation, about 16 minutes has been needed for brine to replace the pore water around the temperature sensors of Port 4 in Run H13-Run H16 with the effects of the different NaCl concentrations at -1 °C. However, the lowest points of temperature have occurred after lapse of time when the replacement had finished. This was caused by salinity change of pore water due to ion diffusion.

Figure 16 gives the curve of the temperature change with time at Ports 1-3 in the vessel in the presence of brine solution with 24 wt% and at -1 °C. As shown in Figure 16, there is a well depth of the temperature change in each temperature curve at Ports 1-3, and the wells appear with time in turn and the depths of the wells from Port 2 to Port 4 gradually increase. In the process of the hydrate dissociation, it might be caused by the direct replacement of pore water with brine at ports 1 and 2, resulting in the thermal homogenization, while the temperature change at Port 4 was caused by salinity change of pore water due to ion diffusion.

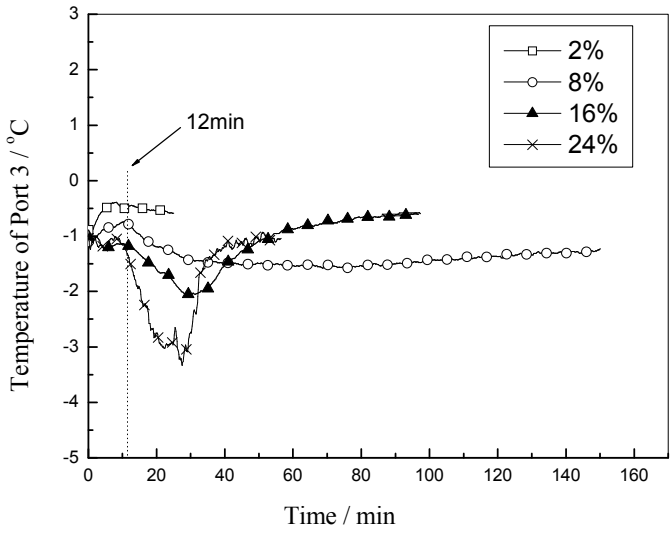

Fig. 3. The curve of the temperature change over time at Port 4 in the vessel in Run H13-Run H16 with the effects of the different brine concentrations at -1 °C

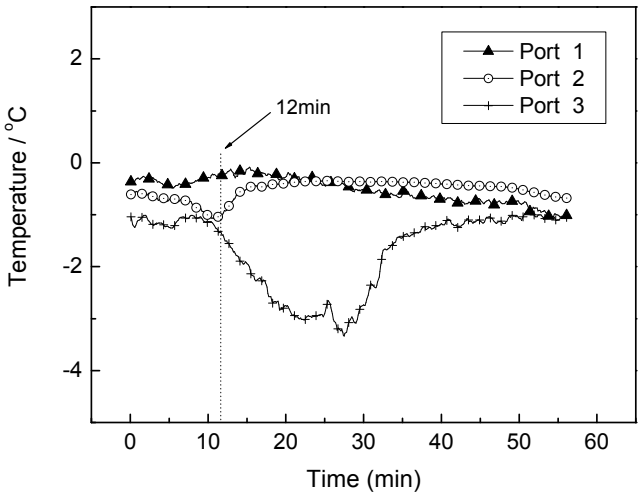

Fig. 4. The curve of the temperature change over time at Ports 1-3 in the vessel in Run H16 with the injection of 24 wt% brine solution at -1 °C

3.2.3 Hot Brine stimulation

Figure 5 gives the typical curve of the temperature change with time at Ports 1-3 in the vessel in the presence of hot brine solution with 24 wt% and at 90 °C. It is shown from the figure that at Port 4, the curve can be divided into three sections: the horizontal section, the downward section and the upward section. The horizontal section represents the non-dissociation and the isothermally endothermal dissociation (phase transformation) processes of the hydrate still without the effect of the inhibitor. The downward section is the cooling endothermal dissociation process of the hydrate on the effects of the hot water and brine solution. In this section, with the increase of concentration of brine solution with time, which acts on the surface of the hydrate, the temperature of the hydrate gradually decreases and the hydrate gradually dissociates until the dissociation is completed while the concentration of brine solution reaches the maximum value. The upward section is only the heterothermally endothermal process of the system in the porous media in the effect of heat after the hydrate dissociation has fully completed. In the section, there are no the phase transformation. As shown in Figure 5 that the characteristics of the temperature changes with Ports 1 and 2 are similar with Port 4. For other salt concentrations and other temperatures of the injected hot solutions, the characteristics of the temperature change are also similar with the above. In addition, as shown in the figure, the flowing of hot brine water injected in the vessel can be also regarded as the moving of a piston from inlet to outlet, as analyzed in Figure 2.

Temperature changes in Port 4 in Run H4, Run H8, Run H12 and Run H16 over time with the injection of the brine of 24 wt% at -1, 50, 90, 130 °C, respectively, have been shown in

Figure 6. The experimental results illustrate that with the brine injected at the same concentrations the same lowest value of temperature decrease of the hydrate system at the same port has been produced and it is independent of the initial temperatures of the injected solutions. The temperature changes over time with the brine injected at the other same concentrations at -1, 50, 90, 130 °C show the similar characteristics.

Figure 7 gives a typical curve of the temperature change over time at Port 4 with Run H1-Run H4 through injecting brine solution with the concentrations of 0, 8, 16, and 24 wt%, respectively, at 130 °C. As shown in Figure 7, it is noted that the time for the hydrate dissociation shortened and the degree of the depth (well depth) of the temperature drop increases with the increase of the concentration of brine solution. For other certain temperatures with the different injections of brine solution of 0, 8, 16 and 24 wt%, respectively, the similar characteristics can be obtained.

The dissociation processes of hydrate have been displayed through temperature curves at various ports changing over time. However, for 2 wt% and 8 wt% salinity curves in Figure 3, temperature shows an increase about 0.2- 0.3 °C during about 2 or 3 minutes early. This is due to heat transfer from the air bath after the air bath had been opened partially to turn on input valve and output valve on the purpose of the injection of liquid as shown in Figure 1. Heat transfer to or from the air bath affected all the temperature measurements during about 2 or 3 minutes early. In spite of that, this increase or drop does not demolish the data explain above because it was much lower than the well depth of the temperature change in the temperature curves occurring later.

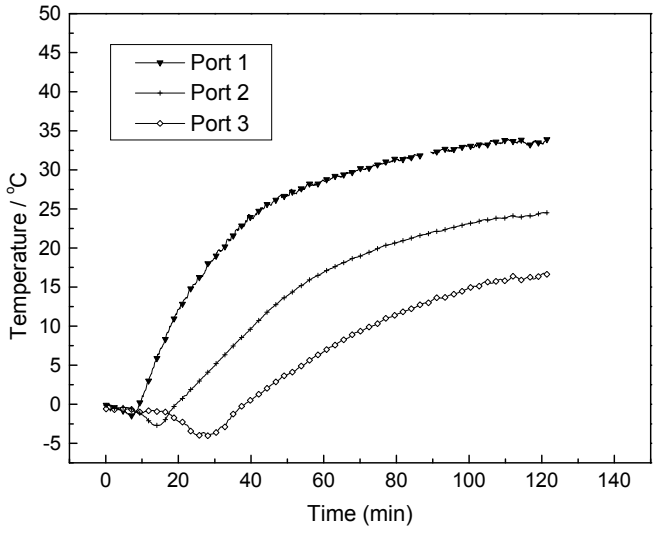

Fig. 5. The curve of the temperature change over time at Ports 1-3 in the vessel in Run H8 with the injection of 24 wt% brine solution at 90 °C

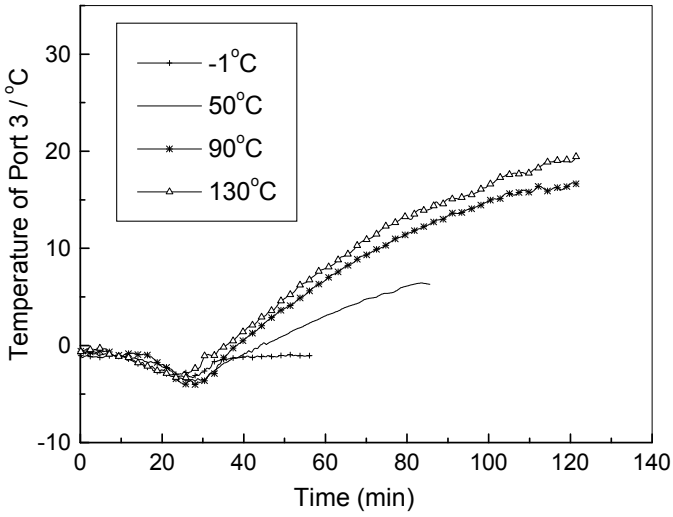

Fig. 6. The curve of the temperature change over time at Port 4 in the vessel in Run H4, Run H8, Run H12 and Run H16 with the injection of 24 wt% brine solution at the different temperatures

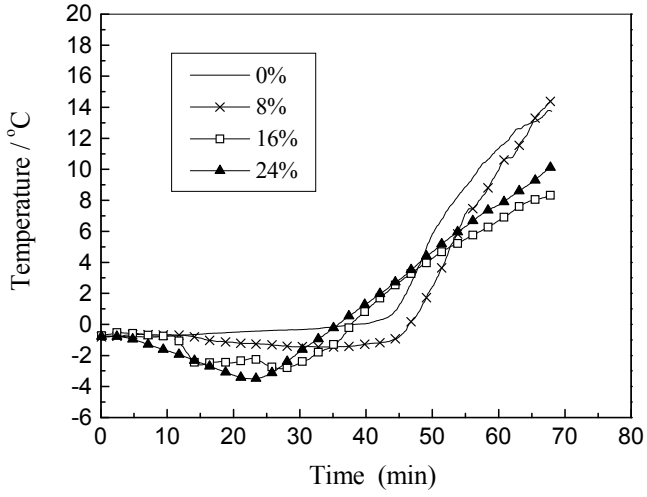

Fig. 7. The curve of the temperature change over time at Port 4 in the vessel in Run H1-Run H4 with the effects of the different brine concentrations at 130 °C.

3.3 Gas production

A typical curve of the accumulative gas production for the whole gas production process in Run H9 is given in Figure 8. As shown in Figure 8, the gas production process with the hot brine or hot water injection in the vessel can be divided into three sections. In Section I, the free methane gas in the vessel is released, and instantaneously gas production rate increases rapidly. The gas production rate could be expressed by the slope of the curve of the accumulative gas production. After the free gas released, the gas production rate decreases remarkably. This section is the hydrate dissociation and gas production process and considered to be Section II. Afterwards in Section III, the hydrate dissociation process has finished, and there is only the residual gas release from the vessel. (Sloan & Koh, 2008) As shown in Figure 8, there are two inflexion points on the curve of the accumulative gas production with time. The left point indicates the end of free gas release process (Section I) and the beginning of the hydrate dissociation process (Section II). The right one means the end of hydrate dissociation process and the beginning of production process of the residual gas (Section III).

Figure 9 gives the accumulative gas production over time with the 2 wt% brine solution injection at -1 ^{o}C, which is a typical case of the gas production without the effects of thermal and brine. It can be seen from the figure that there is only the free gas production without the dissociated gas from the hydrate in this case.

Figure 10 shows the accumulative gas production in Section II with the hot water injection at 50, 90 and 130 ^{o}C, respectively, as did in Run H9, Run H5 and Run H1. The hydrate dissociation rate increases with the increase of the temperature of the injected hot water during the hydrate dissociation process (Goel et al., 2001).

Figure 11 gives the accumulative gas production in Section II at 50 ^{o}C with the injections of the brine solution in the concentration range of 0~24 wt%. The hydrate instantaneous dissociation rate could be increased by injecting brine solution other than water, and it is related to the concentration of injected brine solution. When the brine concentration is less than 16 wt%, the dissociation rate increases with the brine concentration. It is noted that the hydrate instantaneous dissociation rate is approximately the same with the injection of brine solution of 16 wt% and 24 wt% at 50 ^{o}C. In other words, if the brine concentration continues rising after reaching certain value, the concentration has little effect on the hydrate instantaneous dissociation rate. Hence, in the process of hydrate dissociation with the injection of hot brine, it is not necessary to use the brine solution with very high concentrations. The accumulative gas production and the hydrate instantaneous dissociation rate at other certain temperature such as -1, 90, and 130 ^{o}C, with the injections of the brine solution in the concentration range of 0~24 wt% show the similar behavior.

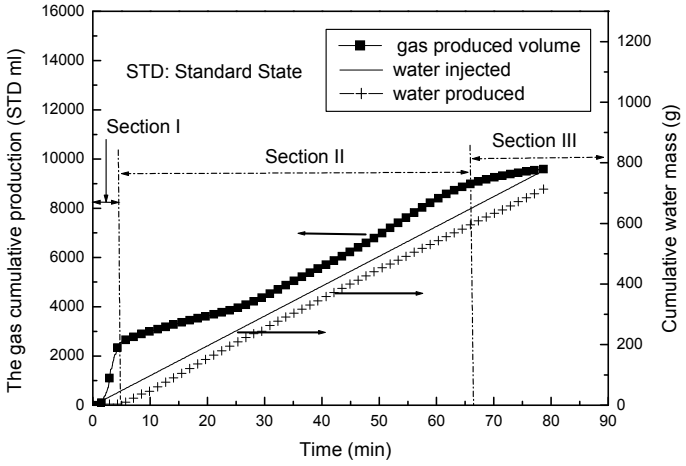

Fig. 8. The accumulative gas production and the accumulative mass of water injected and produced over time in Run H9 with the injection of hot water at 50 ◦C

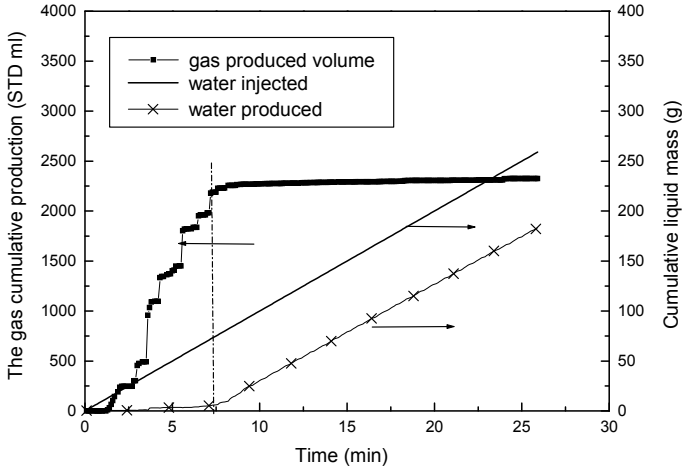

Fig. 9. The accumulative gas production and the accumulative mass of brine injected and produced in Run H13 with the injection of 2 wt% brine solution at -1 ◦C

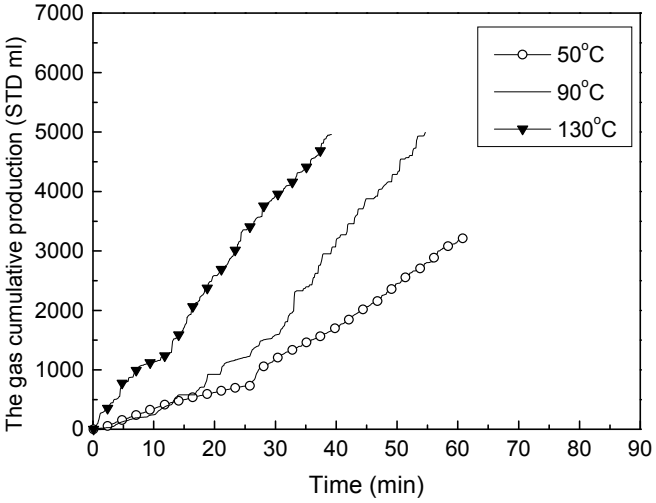

Fig. 10. The accumulative gas production at section II in Run H1, Run H5 and Run H9 with the effects of hot water at 50 °C, 90 °C and 130 °C

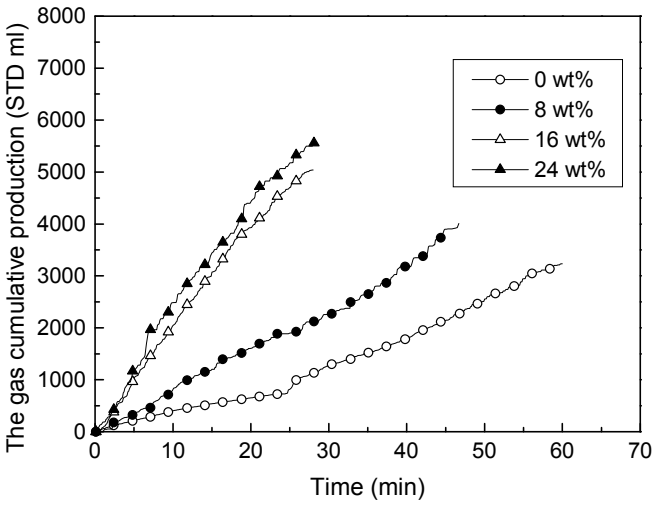

Fig. 11. The accumulative gas production at section II in Run H9-Run H12 with the effects of the different brine concentrations at 50 °C

3.4 Liquid production

As shown in Figure 8, during free gas production, with hot water or hot brine injection there is little liquid production. This stage is one process that free gas in the vessel is drived out, and in this stage, the injected liquid solution stays in the vessel. During the hydrate dissociation, the liquid production rate is slightly higher than the solution injection rate, due to the water produced from the hydrate dissociation. After the hydrate dissociation process finished, the liquid production rate is equal to the solution injection rate.

3.5 Production efficiency analysis

In this work, to determine the efficiency of gas production from the hydrate by hot brine injection, the thermal efficiency and the energy ratio are investigated. The thermal efficiency is defined as the ratio of the heat quantity for hydrate dissociation to the total heat input, which is defined as the amount of heat needed to raise the temperature of the hydrate system in the vessel up to the injection temperature. Thus, when the fluid is injected at 0 °C or less than 0 °C, the thermal efficiency is zero, and there is no thermal effect on the hydrate system in the vessel by the fluid injected. The energy ratio is defined as the ratio of the combustion heat quantity of produced gas to the total input heat quantity (Li et al., 2006, 2008b).

Thermal efficiencies and energy ratios for the hydrate production in the above various experimental runs under hot water and hot brine injections are shown in Figures 12 and 13, respectively. As shown in Figures 12 and 13, the thermal efficiency and the energy ratio decrease with the increase of the temperature of injected hot water at the 0 wt% salinity. For the case of the injection of hot brine solution, the thermal efficiency and the energy ratio increase with the increase of the concentration of injected hot brine with the certain temperature. For hydrate dissociation, more powerful temperature-driving force comes forth resulting from increasing salinity and thus hydrate dissociates more rapidly resulting in smaller the total heat input. Then, increasing thermal efficiency and energy ratio have been obtained.

However, with the differences of the temperatures of the injected hot brine, the degrees of the increases of the thermal efficiency and the energy ratio are different. As shown in Figures 12, 13, it is noted that at low temperature, 50 °C, the increase effectiveness of the thermal efficiency and the energy ratio is apparent with the increase of the concentration of hot brine. Whereas, at high temperature thus as 130 °C, there are only a little increase for them. Hence, it is suggested that in the gas hydrate production by the hot brine injection, the appropriate temperature in conjunction with the high concentration of brine solution brings relative high recovery efficiency. The injection with too high temperature results in the energy loss.

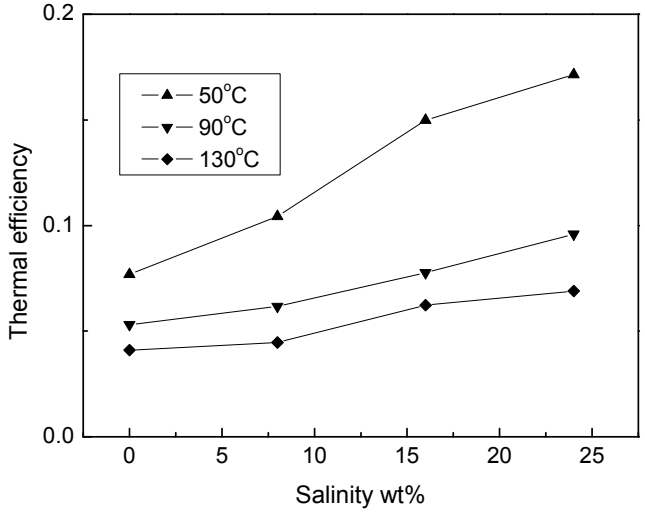

Fig. 12. Thermal efficiencies of gas production with the salinity at 50 °C, 90 °C and 130 °C

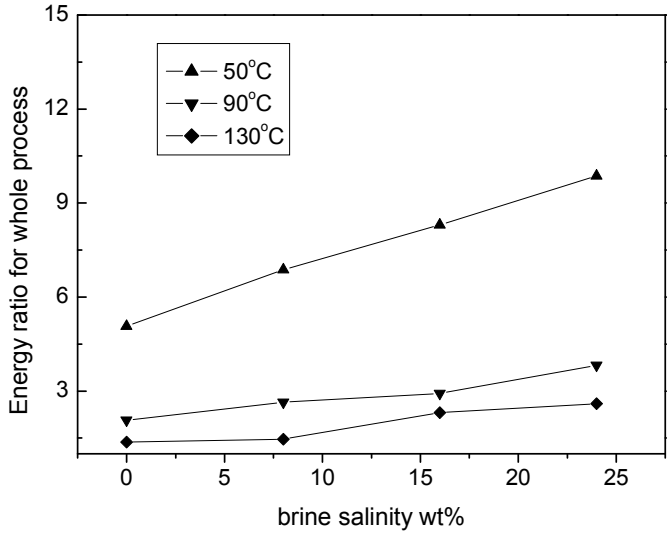

Fig. 13. Energy ratios of gas production with the salinity at 50 °C, 90 °C and 130 °C

4. EG stimulation

4.1 Experimental Procedures

During the experiment, the raw dry quartz sand with the size range of 300-450 μm are tightly packed in the vessel, and then the vessel was evacuated twice to remove air in it with a vacuum pump. The quartz sand in the vessel was wetted to saturation with distilled water using a metering pump. The sand sediment was saturated when the amount of water produced from the vessel was equal to the amount of water injected. It was assumed that the volume of water injected in the vessel was the total volume available in the vessel. Then the methane gas was injected into the vessel until the pressure in the vessel reaches much higher than the equilibrium hydrate formation pressure at the working temperature. After that, the vessel was closed as an isochoric system. The temperature was gradually decreased to form the hydrate by changing the air bath temperature. The hydrate formation was considered to be completed until there was no pressure decrease in the system. The hydrate formation process in general lasts for 2 to 5 days.

The hydrate dissociation by EG injection was carried out in the following procedures. Firstly, the EG solution with the desired concentration was prepared in the middle containers. The back pressure regulator was set to 3.8MPa, which is the system pressure during the hydrate dissociation process under EG injection. Then the dissociation run was started by injecting the EG solution from the middle containers into the vessel. The EG solution was cooled down to the temperature in the air bath before injected into the vessel. After injecting the EG solution for approximately 5 mins, hydrate began to dissociate and gas and water solution were observed to release from the vessel through the outlet valve. The gas production process lasted for 30-100 min, depending on the EG concentrations and injection rates. When there was no significant gas released, the EG injection was finished and the system pressure was released to 1 atm. gradually. During the entire dissociation run, the temperature and pressure in the vessel, the gas production, the amount of EG solution injected and the water production were recorded at 2 seconds intervals.

4.2 Hydrate Formation

Table 2 provides the hydrate formation conditions. The volume of the water and gas before hydrate formation is equal to the total volume of water, gas and hydrate after hydrate formation:

$$V_{w1}+V_{g1} = V_{w2}+V_{g2}+V_{h2} \quad (1)$$

It was assumed that there is 5.75 mol water in 1mol methane hydrate, and the density of methane hydrate is 0.94 g/cm^3 and water in the vessel is incompressible. The volume of the gas in the vessel after hydrate formation was calculated by the pressure and temperature conditions in the vessel using the Peng-Robinson equation. The inlet and outlet pressures of the vessel change simultaneously due to the high porosity and permeability of the sediment, so the pressure in the vessel in this work takes the average of the inlet and outlet pressures.

Figure 14 shows a typical experimental result of the pressure and temperature profiles with time during MH formation in the sediment. It can be seen from Figure 14 that the pressure profile during MH formation could be divided into four sections. In section I (0 min-175 min), the temperature decreased from 17.0 °C to 2.0 °C in isochoric condition, and the pressure decreases from 5.4 MPa to 5.1 MPa due to the gas adsorption on porous the quartz sand and the gas contraction in the vessel. After section I, the closed system was maintained at a constant

temperature (2.0 °C) until the end of the experiment. In section II (175 min-280 min), the pressure of the closed system was above 5.0 MPa, which was much higher than the pure hydrate equilibrium pressure of 3.5 MPa at 2.0 °C. (Sloan & Koh, 2008) This section was considered to be the hydrate nucleation process, and in this period of time there was no hydrate formed in the vessel. (Fan et al., 2006) The section III is the hydrate formation process. In this section, the pressure gradually decreased due to the gas consumption during the hydrate formation, and this section takes much longer time than section I and II. In the last section (section IV), no further pressure decrease was observed, and the system was maintained at a constant temperature. Hence, the system reached the thermodynamic stable state.

Total 7 experimental runs of hydrate dissociation by EG injection have been carried out. Run E0 as the blank experiment, which injected the distilled water instead of EG solution, was used to eliminate the influence of the gas production by the liquid injection. Table 3 provides the experimental conditions during hydrate dissociation by EG injection, including the EG injection rate, the EG concentration and the average pressure and temperature during MH dissociation. The hydrate dissociation runs in Table 3 were related to the formation runs in Table 2.

	experimental runs							
	E0	E1	E2	E3	E4	E5	E6	E7
Initial Pressure (MPa)	5.403	5.519	5.488	5.476	5.306	5.311	5.416	5.409
Initial temperature (°C)	17.83	17.89	18.01	17.71	17.83	17.46	17.77	17.95
Final Pressure (MPa)	3.556	3.502	3.467	3.480	3.557	3.566	3.516	3.486
Final temperature (°C)	1.97	1.92	1.81	1.92	2.00	2.07	1.81	1.73
Final amount of water (ml)	43.73	47.53	46.22	45.53	42.18	41.95	42.92	43.26
Conversion of gas to hydrate (%)	33.03	36.77	36.82	36.22	31.44	31.49	33.83	34.52
Hydrate content (vol, %)	7.33	8.16	8.17	8.04	6.98	6.99	7.51	7.66

Table 2. Formation conditions of hydrate related to hydrate dissociation by EG injection

	experimental runs							
	E0	E1	E2	E3	E4	E5	E6	E7
EG injection rate (ml/min)	8.8	4.9	6.8	8.8	8.8	8.8	8.8	8.8
EG concentration (wt %)	0	30	30	30	40	50	60	70
Pressure (MPa)	3.889	3.862	3.926	3.862	3.864	3.85	3.901	3.825
Temperature (°C)	2.043	1.645	2.015	1.985	2.061	1.901	2.010	1.846

Table 3. Experimental conditions during Hydrate dissociation by EG injection

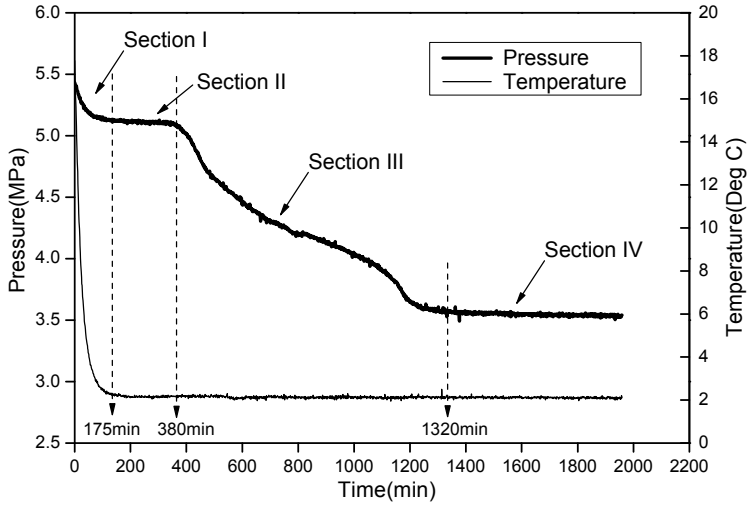

Fig. 14. The pressure and temperature profiles during hydrate formation in isochoric experiment

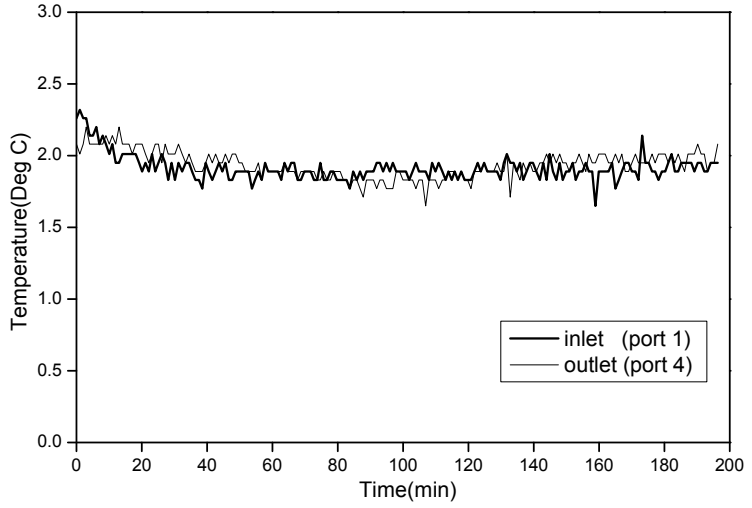

Fig. 15. The inlet and outlet temperature during the EG injection for Run E3

4.2 Hydrate Dissociation

4.3.1 Temperature distribution

Before injected into the vessel, the EG solution was cooled by the coil in the air bath. In an unstirred system, such as the vessel used in the experiment, it is difficult for the methane gas and water to form methane hydrate completely. Hence, only a little hydrate was formed and most part of water or gas was remained in the vessel. Besides, the existing of quartz sand disperses the formed hydrate. Thus, the temperature neither sharply increases in the process of methane hydrate formation shown in Figure 14 nor sharply decreases in the process of methane hydrate dissociation. So the temperature in the vessel maintained constant during EG solution injection.

The inlet (port 1) and outlet (port 4) temperature in the vessel during the EG injection for Run E3 is shown in Figure 15, and the temperature profiles for all other runs show a similar trend with Run3.

4.3.2 Gas and liquid production rate

The gas production rate for whole production process for Run E5, which is a typical one, is shown in Figure 4. The gas production rates for other runs show the similar characteristics.

As shown in Figure 4, the process of the hydrate dissociation with the EG injection in one-dimensional vessel can be divided into four main sections. In section I, the free methane gas in the vessel was released. This caused the sudden increase of instantaneous gas release rate, up to 800 ml/min. After the free gas released, the gas production rate decreased and maintained about 30 ml/min. This section is considered to be section II. In section I and II, the EG was diluted by the remained water in the vessel after hydrate formation, and there were little hydrate dissociated due to the low concentration of EG solutions. With further injection of the EG, the concentration of the EG solution in the vessel increased gradually. The EG is a hydrophilic chemical that lowers the activity of water and destroys the structure of the hydrate. When the EG concentration increased high enough to make the hydrate dissociate, the gas production rate suddenly increased to about 100 ml/min, which indicated that the hydrate in the vessel began to dissociate. This is the hydrate dissociation section (section III). The dissociation section lasted approximately 25 min, which is the longest time among the four sections, as shown in Figure 16. Section IV was the last section of the experiment, with remain gas released.

Table 4 provides the Run Etime and gas produced from hydrate dissociation by EG injection for all runs. The EG injection time is from the beginning of EG injection to the end of hydrate dissociation. Onset time for hydrate dissociation is the starting point of section III, and the duration of hydrate dissociation is the length of time of section III. For example, in Run E5 in Figure 16, the onset time for the hydrate dissociation section is 8 min and the end of this section is 32 min, resulting in the duration of hydrate dissociation of approximately 24 min. The gas production ratio is defined as the ratio of the amount of gas generated from hydrate in the hydrate dissociation section and the initial amount of gas contained in all hydrate excluding the free gas in the vessel. Total gas produced after EG injection is also given in Table 4.

The rate of hydrate dissociation by EG injection is a function of EG concentration, injection rate of EG solution, pressure, temperature of the system and hydrate-EG interfacial area. (Sira et al., 1990) In this work, the pressure, temperature and the EG injection rate maintain

constant after the EG injection. The instantaneous gas production rates during the whole process were unsteady as shown in Figure 16, while the hydrate dissociation rate decreased continuously with time as illustrated by a typical run (Run E5) in Figure 17. The hydrate dissociation rate was calculated by the gas production rate of section III in Figure 16, in which the gas production was caused by the hydrate dissociation at the certain pressure and temperature.

Figure 18 shows the effect of the EG injection rate on the cumulative gas produced from hydrate dissociation as a function of time for Runs 1-3. The cumulative gas produced from the vessel was measured by the gas flow meter in Figure 1. In Runs 1-3, the EG concentration was kept the same at 30 wt% and the injection rate was varied from 4.9 to 8.8 ml/min. As shown in Figure 18, in general, with the increase of the EG injection rate, the cumulative gas produced increased. As the EG injection rate increase, there were more EG injected into the vessel at the same time, which increased the hydrate-EG interfacial area and stimulated more hydrate dissociate at the same time. The general trend for gas production rate profile is similar in Runs 1-3, but the onset time and duration of hydrate dissociation section are all different with different EG injection rate. As shown in Table 4, from Run E1 to Run E3, the duration of hydrate dissociation section decrease from 73 min to 35 min, while the gas production ratio increased from 38.9% to 50.6%.

Figure 19 shows the effect of the EG concentration on the cumulative gas produced from hydrate dissociation as a function of time for fixed injection rate (Runs 3-7). From Runs 3 to 7, the EG injection rate was maintained same at 8.8 ml/min and the EG concentration was varied from 30 to 70 wt%. Run E0 was the blank experiment, which injected the distilled water instead of EG solution, with the same injection rate as Runs 3-7. Although the general trend for gas production rate profile is similar in Runs 3-7 with the same EG injection rate, the duration of hydrate dissociation decrease as the EG concentration increased from 30 wt% to 70 wt%. As shown in Table 4, from Run E3 to Run E7, the gas production ratio increased from 50.6% to 96.2%. The gas production ratio is larger than 90% while the EG concentration is over 60 wt% during hydrate dissociation. On the other hand, the EG injection time for all runs are different, which decreases with the increase of injection rate and concentration of the injected EG solution in general.

The EG injection and the solution production rate profiles are much simpler than that of the gas production, and Figure 20 gives a typical profile (Run E5). The solution produced from the outlet of the vessel was composed of the EG solution, water in the vessel before EG injection, and water produced from the hydrate dissociation. From Figure 20, the EG injection rate kept nearly constant for the whole production process. While there was fluctuation for the solution production rate, due to the unsteady state during hydrate dissociation process under the chemical stimulation.

	experimental runs							
	E0	E1	E2	E3	E4	E5	E6	E7
EG injection time (min)	-	107	71	43	33	32	29	24
Onset time for hydrate dissociation (min)	-	34	21	8	6	8	7	4
Duration of hydrate dissociation (min)	-	73	50	35	27	24	22	20
Gas produced from hydrate (ml)	-	977	1088	1252	1547	1800	2194	2268
Gas production ratio (%)	-	38.9	43.3	50.6	72.1	83.7	95.0	96.2
Gas produced after EG injection (ml)	-	3496	3334	4025	3210	3933	4180	3368

Table 4. Run time and gas produced from hydrate dissociation by EG injection

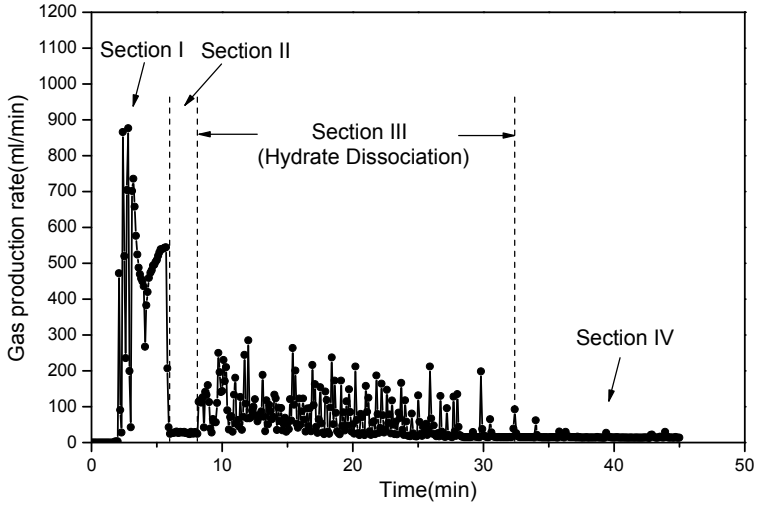

Fig. 16. The gas production rate for Run E5

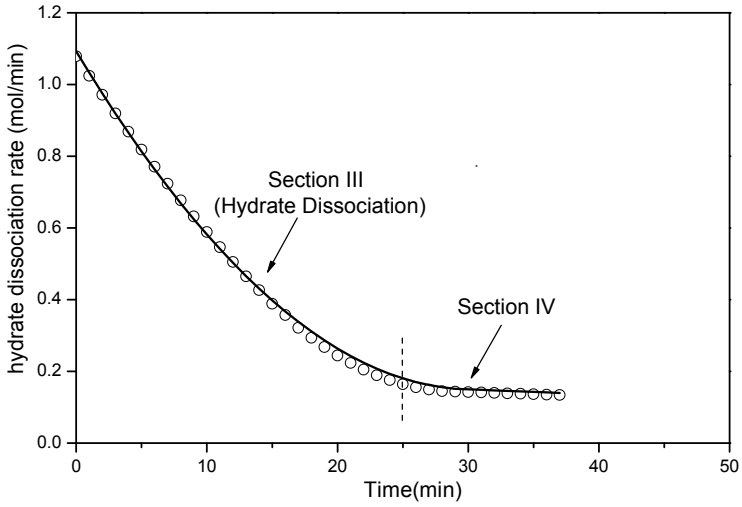

Fig. 17. The hydrate dissociation rate for Run E5

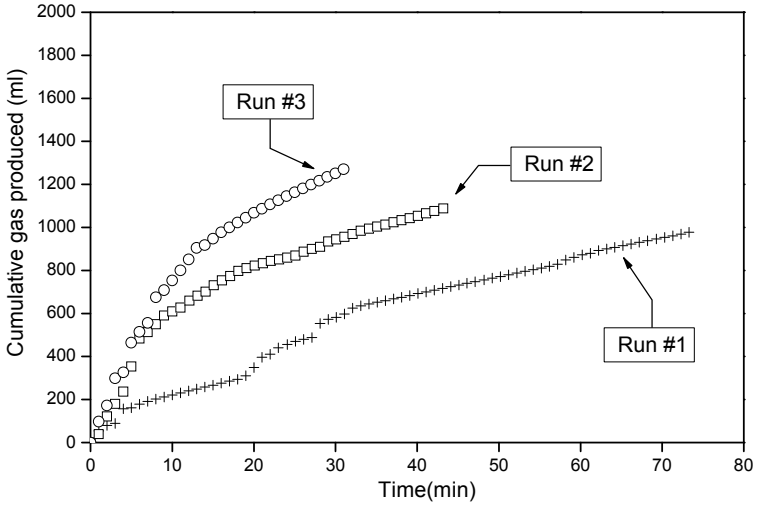

Fig. 18. The cumulative gas produced during the hydrate dissociation for Runs 1-3

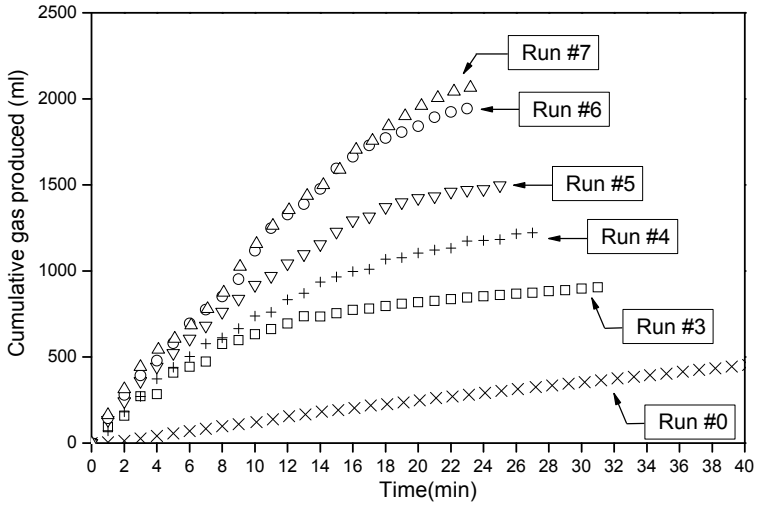

Fig. 19. The cumulative gas produced during the hydrate dissociation for Runs 3-7

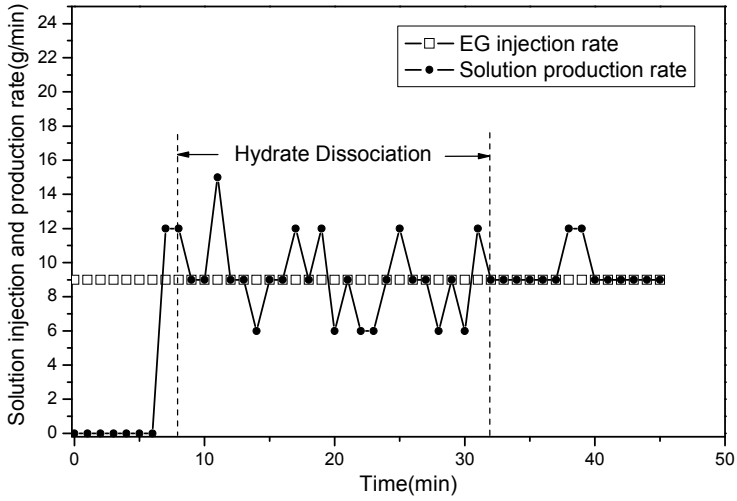

Fig. 20. Solution injection and production rate profile for Run E5

4.3.3 Production Efficiency Analysis

The efficiency of producing gas from hydrate by EG injection is investigated here. In order to compare the efficiency of different runs, the production efficiency has been defined as the ratio of the volume of produced gas to the mass of EG injected in unit time.

Under the EG stimulation, the hydrate dissociated only on the hydrate dissociation section (Section III shown in Figure 16). Table 5 shows three production efficiencies:
1) Production efficiency for hydrate dissociation section (section III) (ml/g/min)
2) Production efficiency at 50% hydrate dissociation (section III) (ml/g/min)
3) Production efficiency for whole injection process (section I to III) (ml/g/min)
The first one was calculated with the volume of gas, the mass of EG injected and the duration time of the hydrate dissociation section (section III in Figure 16). It can be used to measure the gas production efficiency of hydrate dissociation process by the effect of EG in section III.
The second one was calculated the same way with the first one, while it used the values of 50% hydrate dissociation point. In this work, the hydrate dissociation runs were divided into 4 sections, and the hydrate dissociation only happened in section III. The amount of dissociated hydrate was measured by the gas volume released from the vessel in section III. So 100% hydrate dissociation point was the end of section III, when the gas produced from hydrate dissociation all released from the vessel. In the same way, 50% hydrate dissociation point was some time in section III, when 50% gas produced from hydrate dissociation.
Both the first and second production efficiencies were calculated based on the experimental result of section III (the hydrate dissociation section).
The third one was used to measure the whole experimental runs, from the beginning of EG injection to the end of the hydrate dissociation process, which include section I to section III.
The formation conditions of hydrate used in the work was same for all runs, including pressure, temperature, amount of water and the hydrate content in the vessel. For all EG injection runs, the impact of the hydrate content, the amount of water and free gas in the vessel, and the difference of the operating conditions (including the pressure and temperature) during EG injection were all eliminated, while the impact of the EG concentration and injection rate on the production efficiency reflected in Table 5. As shown in Table 5, the production efficiency for the whole EG injection process was between 0.20 and 0.88 ml/g/min, while the efficiency for hydrate dissociation section was between 0.12 and 0.80 ml/g/min. But the production efficiency at 50% hydrate dissociation was much higher, with the maximum of 2.03 ml/g/min.
From the efficiency analysis, the following conclusions can be drawn: (1) the production efficiency of the hydrate dissociation section, 50% hydrate dissociation and the whole injection process varied with the EG concentration and injection rate, and the variation presented the same trend. (2) The hydrate dissociation rate decreased as the experiments go on, as shown in Figure 17. This can explain why the efficiencies at 50% hydrate dissociation were all higher than that of the whole injection process. (3) With the increase of the EG injection rate, the production efficiency increases, as Runs 1-3. The production efficiencies for hydrate dissociation section of Runs 1, 2 and 3 increase from 0.12 to 0.50 when the injection rate increase from 4.9 to 8.8 ml/min. (4) The EG concentration also influence the production efficiency, as Runs 3-7. From the result shown in Table 5, there was a maximum point for the EG concentration on the production efficiency with the same injection rate (9 ml/min), as Run E6 with 60 wt% EG solution. With the increase of the EG concentration, the gas production rate increases, as the result shown in Figure 19. While the mass of EG injected into the vessel increase with the increase of the concentration, the production efficiency reaches the maximum of 0.80 in Run E6. The same result was also concluded on

the production efficiency at 50% hydrate dissociation and the whole production process including the free gas release section.

	experimental runs							
	E0	E1	E2	E3	E4	E5	E6	E7
Production efficiency for hydrate dissociation section (section III) (ml/g/min)	-	0.12	0.28	0.50	0.57	0.60	0.80	0.76
Production efficiency at 50% hydrate dissociation (section III) (ml/g/min)	-	0.44	1.32	1.60	1.61	1.75	2.03	1.53
Production efficiency for whole injection process (section I to III) (ml/g/min)	-	0.20	0.31	0.79	0.79	0.81	0.88	0.86

Table 5. Production efficiency analysis for the hydrate dissociation by EG injection

5. Conclusions

1 The flowing of hot water or hot brine injected in the vessel can be regarded as the moving of a piston from the inlet to the outlet.
2 The hydrate dissociation process is divided into three stages: free gas production, hydrate dissociation and residual gas production.
3 The process of the hydrate dissociation is a process of the temperature decrease in the presence of the brine solution. The duration of the hydrate dissociation is shortened and the degree of the depth of the temperature drop increases with the increase of the brine concentration.
4 The rate of instantaneous hydrate dissociation increases with the increase of brine concentration with the injection of hot brine solution. However, when the brine concentration is higher than the certain degree, the rate of instantaneous hydrate dissociation no longer continues to increases.
5 During the hydrate dissociation, the rate of the liquid production is slightly higher than the rate of the solution injection, due to the water produced from the hydrate dissociation.
6 Thermal efficiency and energy ratio for the hydrate production can be enhanced by injecting hot brine solution, and the enhance effectiveness is apparent with the injection of high brine concentration at the relative low temperature.
7 After the EG injection, the hydrate dissociation in the vessel can be divided into four sections, that is the free gas producing section, EG diluting section, the hydrate dissociating section and the remnant gas producing section.
8 The gas and water production rate were both unsteady during hydrate dissociation rate decrease continuously with time under the EG stimulation, while the EG injection rate kept nearly constant for the whole production process.

9 Under the experiment conditions, with the EG injection rate increasing, the gas production ratio increased, the duration of hydrate dissociation shortened and the production efficiency increased.

10 Under the experiment conditions, with the EG concentration increasing, the gas production ratio increased, the duration of hydrate dissociation process shortened. And the EG concentration also affects the production efficiency. The production efficiency for the whole EG injection process increased with the EG concentration increasing from 0 to 60wt%, and after that the production efficiency began to decrease.

6. Acknowledgments

The authors appreciate the financial support from the National High Technology Research and Development Program of China (No.2006AA09A209, No.2006AA05Z319) and the National Natural Science Foundation of China (No.20676133).

7. References

Collett, T. S. (2004). Gas hydrates as a future energy resource, *Geotimes*, 49, 11, (2004) pp 24-27, ISSN 0016-8556

Fan, S. S.; Zhang, Y. Z.; Tian, G. L.; Liang, D. Q.; Li, D. L. (2006). Natural gas hydrate dissociation by presence of ethylene glycol. *Energy & Fuels*, 20, 1, (2006) pp 324-326, ISSN 0887-0624

Goel, N.; Wiggins, M.; Shah, S., Analytical modeling of gas recovery from in situ hydrates dissociation. *Journal of Petroleum Science and Engineering* 2001, 29, (2), 115-127, ISSN 0920-4105

Kamath, V. A. M., P.N.; Sira, J.H.; Patil, S.L. (1991). Experimental study of Brine injection and depressurization methods for dissociation of gas hydrate. *SPE Formation Evaluation*, 6, 4, (1991) pp 477-484, ISSN 0885-923X

Kawamura, T.; Yamamoto, Y.; Ohtake, M.; Sakamoto, Y.; Komai, T.; Haneda, H. (2005a). Dissociation experiment of hydrate core sample using thermodynamic inhibitors, *15th International Offshore and Polar Engineering Conference (ISOPE 2005)*, pp. 346-350, Seoul, SOUTH KOREA, Jun 19-24, 2005, ISBN 1-880653-64-8

Kawamura, T.; Yamamoto, Y.; Ohtake, M.; Sakamoto, Y.; Komai, T.; Haneda, H. (2005b). In Experimental study on dissociation of hydrate core sample accelerated by thermodynamic inhibitors for gas recovery from natural gas hydrate, *The 5th International Conference on Gas Hydrate*, pp 3023-3028, Trondheim, Norway, 12-16 June, 2005, ISBN 9781615670666

Kawamura, T.; Sakamoto, Y.; Ohtake, M.; Yamamoto, Y.; Haneda, H.; Yoon, J. H.; Komai, T. (2006). Dissociation behavior of hydrate core sample using thermodynamic inhibitor, *International Journal of Offshore and Polar Engineering*, 16, 1, (2006) pp 5-9, ISSN 1053-5381

Kawamura, T.; Ohtake, M.; Sakamoto, Y.; Yamamoto, Y.; Haneda, H.; Komai, T.; Higuchi, S. (2007). Experimental study on steam injection method using methane hydrate core samples, *Proceedings of The Seventh (2007) ISOPE Ocean Mining Symposium*, pp 83-86, Lisbon, PORTUGAL, Jul 01-06, 2007, ISBN 1-880653-57-X

Klauda, J. B.; Sandler, S. I. (2005). Global Distribution of Methane Hydrate in Ocean Sediment, *Energy & Fuels*, 19, 2, (2005) pp 459–470, ISSN 0887-0624

Kono, H. O.; Narasimhan, S.; Song, F.; Smith, D. H. (2002). Synthesis of methane gas hydrate in porous sediments and its dissociation by depressurizing, *Powder Technology*, 122, 2-3, (2002) pp 239-246, ISSN 0032-5910

Li, G.; Tang, L.; Huang, C.; Feng, Z.; Fan, S. (2006). Thermodynamic evaluation of hot brine stimulation for natural gas hydrate dissociation, *Huagong Xuebao/Journal of Chemical Industry and Engineering (China)*, 57, 9, (2006) pp 2033-2038, ISSN 0438-1157

Li, G.; Li, X.; Tang, L.; Zhang, Y. (2007a). Experimental investigation of production behavior of methane hydrate under ethylene glycol stimulation in unconsolidated sediment, *Energy & Fuels*, 21, 6, (2007) pp 3388-3393, ISSN 0887-0624

Li, G.; Li, X.; Tang, L.; Zhang, Y.; Feng, Z.; Fan, S. (2007b). Experimental Investigation of Production Behavior of Methane Hydrate under Ethylene Glycol Injection, *Huagong Xuebao/Journal of Chemical Industry and Engineering (China)*, 58, 8, (2007b) pp 2067-2074, ISSN 0438-1157

Li, X. S.; Wan, L. H.; Li, G.; Li, Q. P.; Chen, Z. Y.; Yan, K. F. (2008a). Experimental Investigation into the Production Behavior of Methane Hydrate in Porous Sediment with Hot Brine Stimulation, *Industrial & Engineering Chemistry Research*, 47, 23, (2008) pp 9696-9702, ISSN 0888-5885

Li, G.; Li, X.; Tang, L.-G.; Li, Q.-P. (2008b). Control Mechanisms for Methane Hydrate Production by Thermal Stimulation, *Proceedings of the 6th International Conference on Gas Hydrates (ICGH 2008)*, Vancouver, British Columbia, CANADA, July 6-10, 2008.

Makogon, Y. F.; Holditch, S. A.; Makogon, T. Y. (2007). Natural gas-hydrates - A potential energy source for the 21st Century, *Journal of Petroleum Science and Engineering*, 56, 1-3, (2007) pp 14-31, ISSN 0920-4105

Milkov, A. V. (2004). Global estimates of hydrate-bound gas in marine sediments: how much is really out there? , *Earth-Science Reviews*, 66, 3-4, (2004) pp 183-197, ISSN 0012-8252

Moridis, G. J. (2003). Numerical studies of gas production from methane hydrates, *SPE Journal*, 8, 4, (2003) pp 359-370, ISSN 0036-1844

Moridis, G. J.; Collett, T. S.; Dallimore, S. R.; Satoh, T.; Hancock, S.; Weatherill, B. (2004a). Numerical studies of gas production from several CH4 hydrate zones at the Mallik site, Mackenzie Delta, Canada. *Journal of Petroleum Science and Engineering*, 43, 3-4, (2004) pp 219-238, ISSN 0920-4105

Moridis, G. J. (2004b). Numerical Studies of Gas Production from Class 2 and Class 3 Hydrate Accumulations at the Mallik Site, Mackenzie Delta, Canada, *SPE Reservoir Evaluation and Engineering*, 7, 3, (2004) pp 175-183, ISSN 1094-6470

Moridis, G. J.; Kowalsky, M. B.; Pruess, K. (2007). Depressurization-induced gas production from class 1 hydrate deposits, *SPE Reservoir Evaluation & Engineering*, 10, 5, (2007) pp 458-481, ISSN 1094-6470

Moridis, G. J.; Collett, T. S.; Boswell, R.; Kurihara, M.; Reagan, M. T.; Koh, C.; Sloan, E. D. (2009a). Toward Production From Gas Hydrates: Current Status, Assessment of Resources, and Simulation-Based Evaluation of Technology and Potential, *SPE Reservoir Evaluation & Engineering*, 12, 5, (2009) pp 745-771, ISSN 1094-6470

Moridis, G. J.; Reagan, M. T.; Kim, S. J.; Seol, Y.; Zhang, K. (2009). Evaluation of the Gas Production Potential of Marine Hydrate Deposits in the Ulleung Basin of the Korean East Sea, *SPE Journal*, 14, 4, (2009) pp 759-781, ISSN 0036-1844

Sira, J. H. Patil, S. L.; Kamath, V. A. (1990). Study of hydrate dissociation by methanol and glycol injection, *Proceedings - SPE Annual Technical Conference and Exhibition*, pp 977-984, Publ by Soc of Petroleum Engineers of AIME, Richardson, TX, USA, 1990.

Sloan, E. D.; Koh, C. A. (2008). *Clathrate Hydrates of Natural Gases*. 3nd ed ed.; Boca Raton, FLorida : Taylor and Francis, Inc.: 2008, ISBN 0-8493-9078

Sung, W. M.; Lee, H.; Lee, C. (2002). Numerical study for production performances of a methane hydrate reservoir stimulated by inhibitor injection, *Energy Sources*, 24, 6, (2002) pp 499-512, ISSN 0887-0624

Sung, W. M.; Lee, H.; Kim, S.; Kang, H. (2003). Experimental investigation of production behaviors of methane hydrate saturated in porous rock, *Energy Sources*, 25, 8, (2003) pp 845-856, ISSN 0887-0624

Tang, L.; Xiao, R.; Huang, C.; Feng, Z.; Fan, S. (2005a). Experimental investigation of production behavior of gas hydrate under thermal stimulation in unconsolidated sediment, *Energy & Fuels*, 19, 6, (2005) pp 2402-2407, ISSN 0887-0624

Tang, L. G.; Li, G.; Hao, Y. M.; Fan, S. S.; Feng, Z. P. (2005b). Effects of salt on the formation of gas hydrate in porous media, *The 5th International Conference on Gas Hydrate*, pp 155-160, Trondheim, Norway, 2005, ISBN 9781615670666

Tang, L.; Li, X.; Feng, Z.; Li, G.; Fan, S. (2007). Control mechanisms for gas hydrate production by depressurization in different scale hydrate reservoirs, *Energy & Fuels*, 21, 1, (2007) pp 227-233, ISSN 0887-0624

Yousif, M. H.; Li, P. M.; Selim, M. S.; Sloan, E. D. (1990). Depressurization of natural gas hydrates in Berea sandstone cores, *J.Inclusion Phenom&Mol Recognition Chem*, 8, (1990) pp 71-88, ISSN 0923-0750

Yousif, M. H.; Abass, H. H.; Selim, M. S.; Sloan, E. D. (1991a). Experimental and theoretical investigation of methane-gas-hydrate dissociation in porous media, *SPE Reservoir Engineering*, 6, 4, (1991) pp 69-76, ISSN 0885-9248

Yousif, M. H.; Sloan, E. D. (1991b). Experimental Investigation of Hydrate Formation and Dissociation in Consolidated Porous Media, *SPE Reservoir Engineering*, 11, (1991b) pp 452-458, ISSN 0885-9248

Fuel Injection
Edited by Daniela Siano

ISBN 978-953-307-116-9
Hard cover, 254 pages
Publisher Sciyo
Published online 17, August, 2010
Published in print edition August, 2010

Fuel Injection is a key process characterizing the combustion development within Internal Combustion Engines (ICEs) and in many other industrial applications. State of the art in the research and development of modern fuel injection systems are presented in this book. It consists of 12 chapters focused on both numerical and experimental techniques, allowing its proper design and optimization.

How to reference
In order to correctly reference this scholarly work, feel free to copy and paste the following:

Xiaosen Li and Gang Li (2010). Experimental Investigations into the Production Behavior of Methane Hydrate in Porous Sediment under Ethylene Glycol Injection and Hot Brine Stimulation, Fuel Injection, Daniela Siano (Ed.), ISBN: 978-953-307-116-9, InTech, Available from: http://www.intechopen.com/books/fuel-injection/experimental-investigations-into-the-production-behavior-of-methane-hydrate-in-porous-sediment-under

INTECH
open science | open minds

InTech Europe
University Campus STeP Ri
Slavka Krautzeka 83/A
51000 Rijeka, Croatia
Phone: +385 (51) 770 447
Fax: +385 (51) 686 166
www.intechopen.com

InTech China
Unit 405, Office Block, Hotel Equatorial Shanghai
No.65, Yan An Road (West), Shanghai, 200040, China
中国上海市延安西路65号上海国际贵都大饭店办公楼405单元
Phone: +86-21-62489820
Fax: +86-21-62489821